CH-99-6-2 (RP-811)

Comparison of Various Methods to Distribute Supply Air in Industrial Facilities

Allan T. Kirkpatrick, Ph.D., P.E.
Member ASHRAE

Kurt Strobel

ABSTRACT

The evaluation of the ventilation effectiveness and thermal comfort for various industrial ventilation schemes has been carried out by scale model experimentation. Forty experiments involving ten ventilation arrangements, each with three supply airflow rates and two possible industrial process heat loads, were performed. Measurements of airspeed, temperature, and contaminant concentration allowed the thermal comfort and contaminant removal to be quantified using the ISO Comfort Standard ISO-7730 and the ventilation effectiveness indices, respectively. Archimedes number scaling was used to convert the small-scale measurements to full-scale conditions.

The largest ventilation effectiveness occurred for a low supply/high return configuration, with values above 1.6, followed by a high supply/high return configuration with values in the range from 1.0 to 1.2. A low supply/low return configuration had values of about 1.0. The ventilation efficiency generally increased when the heat load was increased and/or the flow rate decreased. Increasing the number of diffusers in the occupied zone increased the ventilation effectiveness. The thermal comfort results depended on the diffuser configuration and the activity level of the worker. Most of the configurations produced acceptable thermal comfort results for a seated worker and unacceptable conditions at an increased activity and clothing level.

INTRODUCTION

The subject of this paper is the experimental determination of the ventilation and thermal comfort performance of a variety of configurations of industrial ventilation systems. The ventilation of industrial facilities is important for two main reasons. One is to maintain thermal comfort. A ventilation system should be designed to remove heat and contaminants added to the working environment by machinery and occupants without overcooling or creating drafts. The second reason that the ventilation of industrial spaces is important is to ensure a supply of fresh air. The introduction of fresh air by a mixing ventilation system reduces the level of contaminants produced by machinery and occupants.

Industrial facilities house large process equipment, with large releases of process heat and contaminants. The spaces in which the equipment is contained are large, with ceilings typically 20 ft (6.1 m) or more above the work floor. The zone of interest for ventilation and thermal comfort is termed the "occupied zone," a volume occupied by people working on the process equipment. The size of the occupied zone in an industrial facility is typically taken as 10 ft (3.0 m) high and 2 ft (0.61 m) from each wall.

There are many configurations of ventilation air distribution systems and a wide range of potential processes in industrial facilities. The industrial ventilation designer must select the size and number of supply and return air outlets and their location in the space. The selection process includes considerations of both ventilation effectiveness and thermal comfort. The type of ventilation process examined in this paper is mixing ventilation, in which the fresh and cool ventilation air will mix with the existing room air, as opposed to displacement ventilation, in which the ventilation system is designed to displace the room air with fresh air.

The impact of the process equipment on the ventilation performance and thermal comfort is not well understood. The objective of this research is to experimentally determine the

Allan T. Kirkpatrick is a professor in the Mechanical Engineering Department, Colorado State University, Fort Collins, Colo. **Kurt Strobel** is an engineer with Advanced Energy, Fort Collins, Colo.

ventilation and thermal comfort characteristics of a scale model industrial space containing process equipment. Specific goals are to compare the performance of supply and return diffusers located at different heights for a range of flow rates and heat loads.

SCALE MODEL TESTING

A one-quarter scale experiment was used in this research. The nondimensional parameters that are applicable to the scaling of an industrial ventilation problem are the Reynolds number, the Archimedes number, and the Prandtl and Schmidt numbers. If all of the similarity parameters between the full-scale prototype and the small-scale model are equal, then complete similarity is satisfied and the small-scale model will accurately predict full-scale conditions. Unfortunately, complete similarity is impossible for the study of indoor ventilation, as both Reynolds number and Archimedes number similarity cannot be satisfied. Howe er, if the Reynolds number is above a critical value, the flow in the scale model becomes independent of Reynolds number. In addition, since the working fluid is air, the Prandtl and Schmidt numbers are the same for the small and full scale.

The Archimedes number was chosen as the small- and full-scale similarity parameter. It is the primary determinant of the flow pattern for a buoyant flow in an enclosure. The Archimedes number is a ratio of the buoyancy and inertial forces and is defined as

$$\mathrm{Ar} = \frac{gL\Delta T\beta}{u^2} \tag{1}$$

where g is the local gravitational acceleration, L is a characteristic length, ΔT is the temperature difference between the supply air and the room air, b is the volumetric thermal expansion coefficient, and u is a characteristic velocity. In this research, the characteristic similarity between a small-scale model (m) and a full-scale prototype (f) requires that the Archimedes numbers be equal for both model and prototype. Assuming that $g_m = g_f$, $\beta_m = \beta_f$, and $\Delta T_m = \Delta T_f$, the Archimedes number similarity requires that

$$\left(\frac{L}{u^2}\right)_m = \left(\frac{L}{u^2}\right)_f \longrightarrow \frac{u_m}{u_f} = \left[\frac{L_m}{L_f}\right]^{1/2} \tag{2}$$

Thus, Archimedes number similarity requires that the small-scale/full-scale air velocity ratio scale as the square root of the small-scale/full-scale geometry ratio. For a geometry ratio of 1/4, the velocity ratio is 1/2, i.e., at geometrically similar locations in the space, the small-scale velocity is 1/2 of the full-scale velocity. Consequently, in the small-scale model, the flow rate per unit floor area and the thermal loading per unit floor area are both 1/2 of the corresponding full-scale values.

VENTILATION AND THERMAL COMFORT INDICES

The contaminant removal or ventilation effectiveness (VE) at a point p in a mechanically ventilated space is (Skaret and Mathisen 1983)

$$VE_p = \frac{C_e}{C_p} \tag{3}$$

where C_e is the contaminant concentration of the exhaust air and C_p is the concentration at a point in the space. This formula is valid when the contaminant concentration of the supply is zero. When there is a nonzero contaminant concentration in the supply, as for the experiments done for this paper, the above equation must be reformulated as

$$VE_p = \frac{(C_e - C_s)}{(C_p - C_s)} \tag{4}$$

where C_s is the concentration of the supply air.

As can be seen from the equation for ventilation effectiveness, point concentrations lower than the exhaust concentration lead to high VE. Obviously, a point located in the supply jet would have a very low contaminant concentration. This would lead to a very high VE. Point concentrations higher than the exhaust concentration lead to low VE. This might occur for points located near a contaminant source. A VE equal to or greater than one is considered desirable. This ensures that the contaminant concentration at the point of interest is lower than that of the exhaust.

An analogous parameter is the temperature effectiveness (TE). This parameter is the ratio of the supply/exhaust temperature difference to a local point/supply temperature difference:

$$TE_p = \frac{(T_e - T_s)}{(T_p - T_s)} \tag{5}$$

A temperature effectiveness of one indicates that the room is well mixed, greater than one indicates that the local point temperature is less than the exhaust temperature, and less than one indicates that the local point temperature is greater than the exhaust temperature. The reciprocal of the temperature effectiveness is the relative stratification of the occupied zone.

The thermal comfort model used in this work is ISO comfort standard 7730 (ISO 1984). This model includes the following parameters: the occupied zone air temperature, airspeed, mean radiant temperature, humidity, and the occupant clothing, metabolic rate, and external work. This model is based on an energy balance on the occupant and includes occupant respiration and perspiration in the energy balance. The output of the model is the predicted mean vote (PMV) and the associated percent persons dissatisfied (PPD). If the PPD is less than 20%, then the thermal conditions are judged to be

acceptable, since at least 80% of the occupants find the thermal conditions acceptable. Int-Hout (1990) has modified the ISO 7730 model to include skin wettedness. It should be noted that the PMV model predicts the thermal sensation for the person as a whole and does not predict local discomfort due to spatial temperature gradients.

The ISO thermal comfort model also requires an occupant clothing and metabolic level. In the research, two different levels of clothing and metabolic activity conditions were chosen and termed "ppd-1" and "ppd-2," as indicated in Table 1. The ppd-1 condition is a typical condition for light industrial work, such as seated assembly or computer work in which the person is sitting and wearing a shirt and pants. The second condition, ppd-2, is also a common industrial condition. It corresponds to heavier industrial work requiring standing and a higher degree of physical activity, such as machining and large-scale assembly. It also assumes that one is working in conditions that require an additional gown worn over the shirt and pants. One met is the rate of energy production per unit area of a seated person at rest. The relative humidity was assumed to be constant at 50%. The mean radiant empera ure was assumed to be the same as the average occupied zone temperature.

TABLE 1
Clothing and Activity Level for Thermal Comfort Model

Condition	Clothing (clo)	Activity Level (met)
ppd-1	0.8	1.2
ppd-2	1.3	2.0

PREVIOUS WORK

Timmons (1984) tested small- and intermediate-sized room models and a full-scale prototype with isothermal flow conditions. He found that above a threshold Reynolds number, the dimensionless velocities and flow pat erns are independent of Reynolds number. The critical Reynolds number was dependent on the room size. Fissore and Liebecq (1991) used a 1:3 scale model to predict velocity distribution and thermal comfort in a slot ventilated space. For two-dimensional flow, they found that the critical Reynolds number was 1,850. Chan et al. (1993) used measurements made on a 1:5 scale model to predict HVAC system performance in a prototype. The experiments were isothermal and satisfied flow rate and air change coefficient similarity. The critical Reynolds number was assumed to be approximately 5,300 based on a stability analysis of flow ina channel reported by Schlicting (1979). They report a general agreement between the airflow patterns of the model and prototype.

Zhang et al. (1993) tested both a model and a prototype with nonisothermal flow. Based on the work of Timmons (1984), Zhang et al. used the prediction that above the threshold Reynolds number, the flow would be independent of the Reynolds number. Zhang et al. found that the model predicted the mean velocity and temperature of the prototype to within 11% and 15%, respectively. Irwin and Besant (1994) investigated contaminant removal by two ventilation systems in a 1:2.5 scale model piggery barn. Similar to the model industrial processes used for this repor , Irwin and Besant used model pigs to generate heat and contaminants. The Reynolds number for the room was not considered a sensitive parameter. The lowest jet Reynolds number they used was approximately 400.

Heiselberg (1996) reported measurements of local ventilation effectiveness with a high supply and high exhaust. Numerical models have also been used for the determination of thermal comfort and ventilation efficiency; see, for example, Chen et al. (1992) and Yaghoubi et al. (1995). However, many of these studies are for typical office spaces, not industrial spaces with large processes.

DESCRIPTION OF EXPERIMENT

The experiments were performed at a university in an instrumented test room. The dimensions of the test room are 15 ft × 25 ft, with a ceiling height of 9 ft (4.6 m × 7.6 m × 2.7 m). With a geometric scale of 1/4, the test cell corresponds to a full-size industrial environment with floor dimensions of 60 ft × 100 ft and a ceiling height of 36 ft (18.2 m × 30.4 m × 11 m). The test room's occupied zone, i.e., that space occupied by workers, is the space 2.5 ft (0.76 m) above the floor and 6 in. (0.15 m) from each wall.

Ten ventilation configurations, two industrial process configurations, and five airflow rate/heat load combinations were tested. The geometries were chosen to provide a simple benchmark comparison of widely used configurations. As shown in Figures 1, 2, and 3, there were four main ventilation configurations.

- Single Wall (SW): two wall grilles located on a single wall
- Opposite Wall (OW): four wall grilles on opposing walls
- Column Drop (CD): two columns in the space, each with two diffusers
- Round (R): two circular diffusers located in the ceiling

These four arrangements have different diffuser throw leng hs. The single wall configuration requires a throw length of the entire room, while the opposite wall configuration requires a throw of half the room length, and the column drop and round configurations require a throw of only a quarter of the room length.

Each of these configurations, with the exception of the round ceiling diffusers, had three height arrangements.

- High supply/high exhaust (HH)
- Low supply/high exhaust (LH)
- Low supply/low exhaust (LL)

The three heightarrangements are illustrated in Figures 1, 2, and 3. The circular ceiling diffuser configuration was used only with a high supply/high exhaust. The supply and exhaust

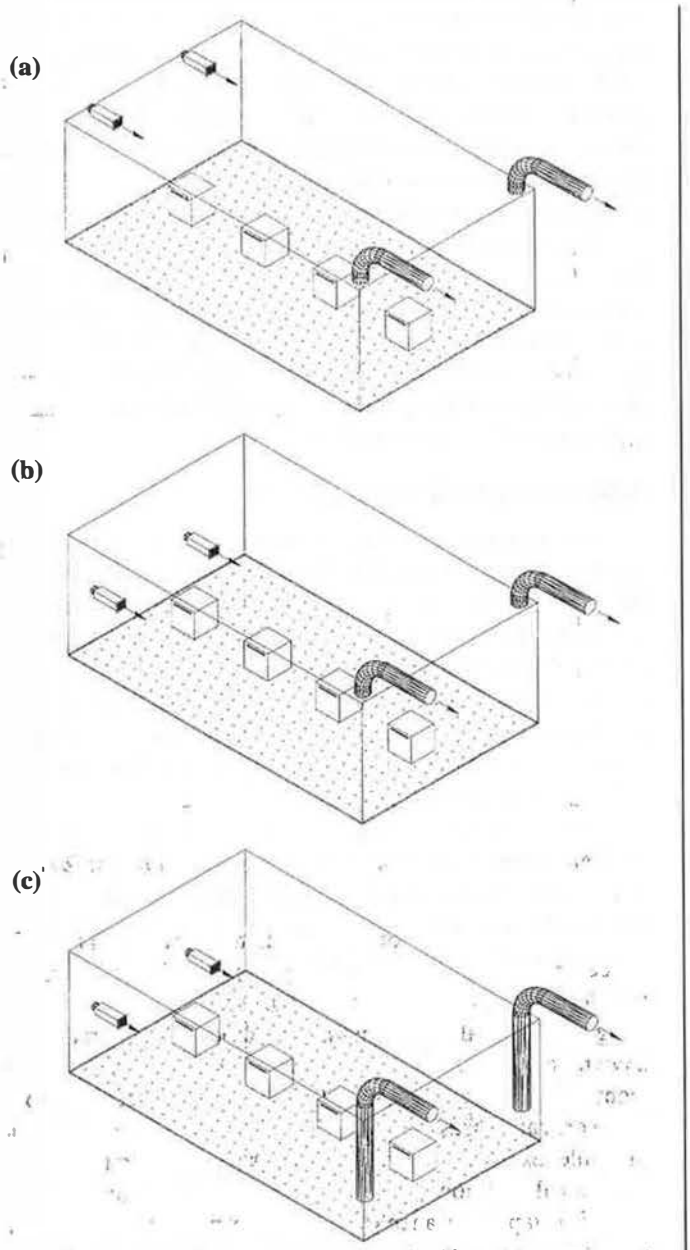

Figure 1 Single wall configuration. (a) Single wall grille, high-high; (b) single wall grille, low-high; (c) single wall grille, low-low.

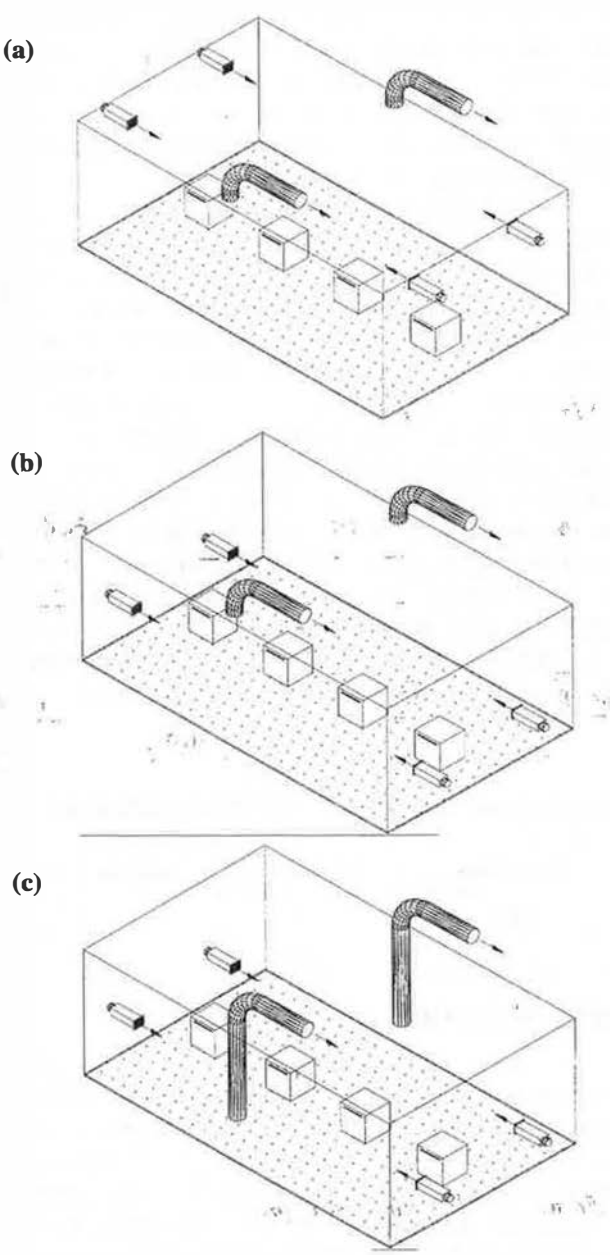

Figure 2 Opposite wall configuration. (a) Opposite wall grille, high-high; (b) opposite wall grille, low-high; (c) opposite wall grille, low-low.

heights for the small-scale experiment are tabulated in Table 2, along with the corresponding full-scale values.

The industrial processes were modeled with 2 ft cubes constructed from sheet metal, as shown in Figure 4. The cube size corresponds to 8 ft × 8 ft × 8 ft (2.4 m × 2.4 m × 2.4 m) full-scale processes. The processes were modeled not as specific industrial processes but as generic processes through which room air was circulated and which released heat and contaminants. The heat source in the cube was an internal electric heater with a constant velocity fan. The heaters had a maximum power output of 1500 W. The power output was controlled by variable voltage supplies and was checked by simultaneous voltage and current measurements.

As shown in Figure 4, each cube had an open slot 1.5 in. high by 1 ft wide located on the bottom of the back side of the cube to serve as an air inlet. Each cube also had an open slot, of the same dimensions, on either side and 2 in. from the top to serve as air and contamination outlets. The contamination source was CO_2 gas. The CO_2 was introduced into the heated flow using a perforated ping pong ball so that it was well mixed with the heated flow inside the cube.

Depending on which ventilation configuration was used, one of two industrial process configurations was used: line or

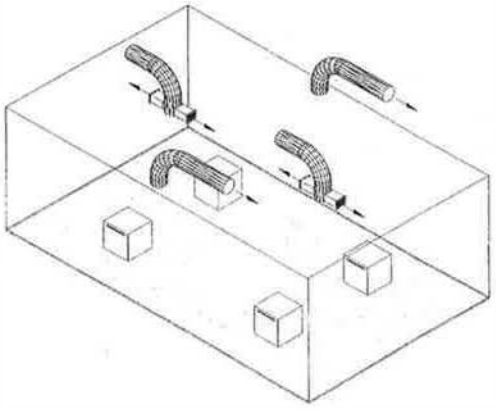

Figure 3 Column drop and wall configuration.

TABLE 2
Supply and Exhaust Heights for Small and Full Scale

	Supply		Exhaust	
	Low ft (m)	High ft (m)	Low ft (m)	High ft (m)
Small Scale	2.5 (0.76)	7.5 (2.3)	2.5 (0.76)	9.0 (2.7)
Full Scale	10.0 (3.0)	30 (9.1)	10.0 (3.0)	36 (11)

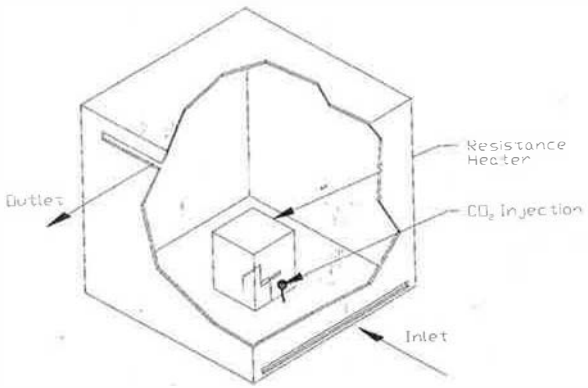

Figure 4 Model industrial process.

centroids, as shown in Figure 5. For the single wall and opposite wall ventilation configurations, a line configuration was used. The line configuration had all four processes along the east-west centerline of the room, one process being located at the center of each quarter of this line. For the column drop and round ventilation configurations, a centroid configuration was used. The centroid configuration had one process located at the center of each quarter of the room. These arrangements ensured that the supply air would be directed into the areas adjacent to the processes where the occupants would be working. The test-cell measurements were made in two planes: the diffuser plane and a center plane perpendicular to the diffuser plane. These planes were chosen as they would be the occupied planes. The measurement planes for both the centroid and line process configurations are shown in Figure 5.

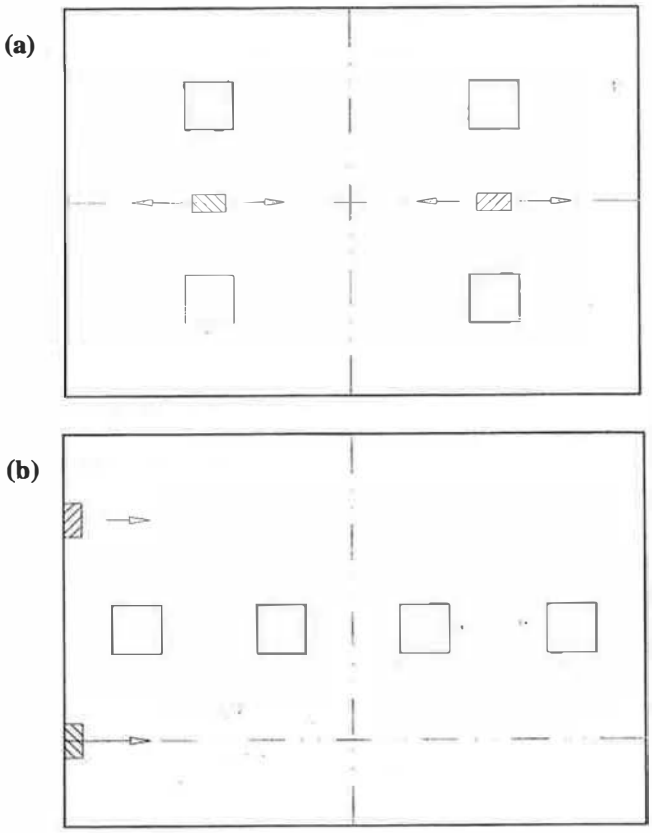

Figure 5 Process configurations. (a) Centroids; (b) line.

All of the test room airspeed, temperature, and CO_2 concentrations were measured by a movable test stand to which all instrumentation was attached. This test stand was hung from a small platform that could be remotely moved to anywhere within the test cell. As shown in Figure 6, measurements were taken at 12 in. (0.30 m) horizontal intervals along the vertical diffuser plane. The instrumentation on the movable test stand included four constant-temperature omnidirectional anemometers, nine thermocouples, and one air sampling tap. The anemometers were positioned at small-scale heights of 6 in., 14 in., 22 in., and 30 in. (15 cm, 36 cm, 56 cm, and 76 cm). Also at each of these four heights, a type-T thermocouple was located for air temperature measurements. The other five thermocouples (also type-T) were located at small-scale heights of 3.75 ft, 5.0 ft, 6.25 ft, 7.5 ft, and 8.75 ft (1.14 m, 1.52 m, 1.91 m, 2.29 m, 2.67 m). Finally, a concentration air sample tap was positioned at a height of 15 in. (0.38 m), equivalent to the 60 in. (1.5 m) height of the full-scale breathing zone.

The HVAC system shown in Figure 7 consisted of an air-handler unit, two heaters, and a system of ducts. The system was designed to supply air from the outdoors and exhaust only to the outdoors, with no internal recirculation. The air inlet and exhaust were located on opposite sides of the laboratory building to minimize contamination of the intake flow by the exhaust stream. The wall grilles had inner dimensions of 5.5 in.

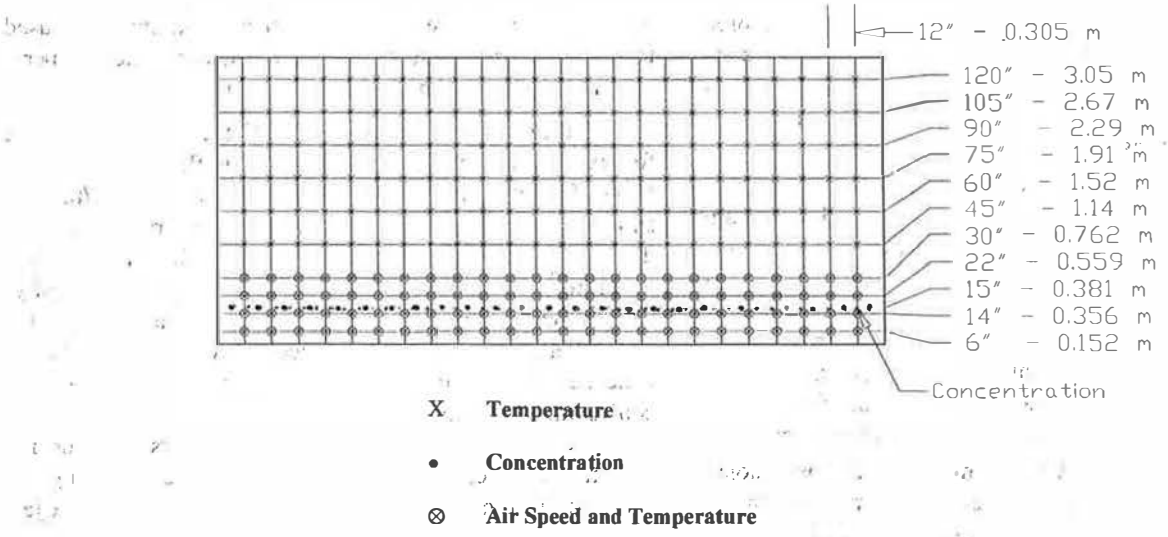

Figure 6 *Data acquisition grid.*

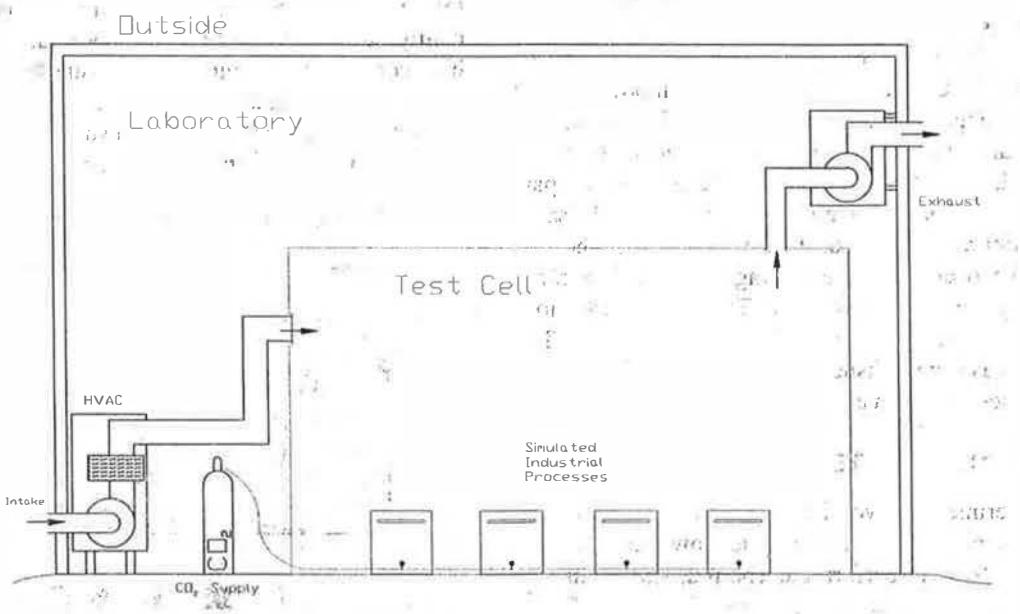

Figure 7 *HVAC system.*

×7.5 in., and the round ceiling diffusers were of 12 in. diameter. The return grilles were two 12 in. diameter ducts attached to an exhaust fan box in one of the laboratory windows.

The airflow rates into the test room were measured using orifice plates and pressure taps connected to a pressure transducer. All airflow rates were calibrated using a 17-point velocity profile integration. The supply air temperature was measured using type-T thermocouples placed upstream of each diffuser. The air inlet was also equipped with a concentration sample tap. The exhaust was equipped with a type-T thermocouple and a concentration sample tap. The temperature of each wall, including ceiling and floor, was measured by a type-T thermocouple located at the center of each wall. The CO_2 concentrations were measured using a nondispersive infrared detector (NDIR) CO_2 analyzer.

As a means of determining experimental accuracy and control, the same test was run three times on three separate occasions. The test case examined was an opposite walls ventilation configuration with low inlet and high exhaust using a small-scale flow rate/heat load combination of 1.0 cfm/ft^2 and 20.4 Btu /h·ft^2. The deviations were between 4% and 6%.

The experimental method used for the tests involved allowing for the development of steady-state conditions, upon arrival at which data could be taken. A test would begin in the morning by turning on the air handler and heaters to their proper settings. Steady thermal conditions would then evolve throughout the next four to five hours. In the early afternoon, the CO_2 supply would be turned on. After an hour, steady contaminant conditions would be present. Upon reaching steady thermal and contaminant conditions, data acquisition would begin. During the data acquisition, all test parameters,

such as supply temperature and flow rate, would be monitored for constancy. For example, the supply air temperature was not allowed to vary more than about 1°F. A lack of constancy in any of these parameters would lead to the dismissal of data and the need to run the test again.

A number of environmental test parameters were recorded before and after each test. These parameters included room conditions (wall, room center, supply, and exhaust temperatures and exhaust, background, and room center CO_2 concentrations) and ambient conditions (atmospheric pressure, outdoor, wet-bulb temperatures). Also among the ambient conditions was the measurement of outdoor background CO_2 concentration. As this concentration remained nearly constant, it was used as a check of the CO_2 analyzer's calibration.

The period over which test cell measurements were done lasted from one to two hours depending on the ventilation configuration. The experimental measurements of occupied zone temperature and velocity in the plane of the diffuser were averaged to determine an average occupied zone temperature and velocity for a given flow rate and load.

The measured supply temperatures for the 40 experiments were not all the same. Since the ISO model uses an energy balance approach, the actual value of the occupied zone temperature will influence the heat transfer from the occupant and, thus, the PPD. In order to do a u iform comparison of the various supply and return configurations, the same supply temperature is required. This was accomplished by normalizing the occupied zone average temperature for a constant supply temperature of 60°F. This corresponds to a 55°F supply temperature with a 5°F duct heat gain. The normalization was accomplished using the measured temperature effectiveness for each experiment.

EXPERIMENTAL RESULTS

Forty experiments involving nine to ten ventilation arrangements, each with three supply airflow rates and two process heat loads, were performed. The four supply airflow rates and heat load combinations are shown in Table 3. These four combinations were chosen on the basis of providing representative room-supply temperature differences from 8°F to 16°F (4°C to 9°C).

The Archimedes numbers of the tests range from approximately 2×10^{-3} to 80×10^{-3}, a relatively negatively buoyant flow regime. The diffuser Reynolds numbers range from 8,100 to 52,000, above the critical Reynolds numbers referenced in the literature review. The length scale in the Archimedes and Reynolds numbers is the diffuser hydraulic diameter. The average temperature in the diffuser plane is used to calculate the representative room-diffuser outlet temperature difference term in the Archimedes number.

TABLE 3
Full-Scale Flow Rate and Heat Load Combinations

Heat Load Btu/h·ft² (W/m²)	Flow Rate cfm/ft² (L/s m²)		
	1.0 (5.1)	2.0 (10.2)	3.0 (15.3)
20 (65)	xx	xx	
40 (130)		xx	xx

The temperature and velocity profiles in the diffuser plane for six representative cases at a full-scale flow rate of 2 cfm/ft² (10 L/s m²) and heat load of 40 Btu/h·ft² (130 W/m²) are shown in Figures 8 through 13. The figures are labeled with the small-scale flow rates and heat loads, which are one-half of the full-scale values. With the single wall high-high configuration, with one diffuser in the measurement plane, the supply jet descends into the space and enters the occupied zone near the center of the room. With the opposite wall configuration, there are two diffusers in the measurement plane, reducing the outlet velocity. The diffuser jets do not penetrate as deeply into the occupied zone, reducing the airspeed and temperature differences compared to a single jet.

The column drop configuration has four diffusers in the measurement plane, further reducing the outlet velocity and the jet penetration into the occupied zone. The low-high configurations are more thermally stratified than the high-high configurations since the cold supply jet is introduced at a lower level. With the low-high configurations, the supply jet is located in the occupied zone, resulting in much larger occupied zone velocities and lower zone temperatures.

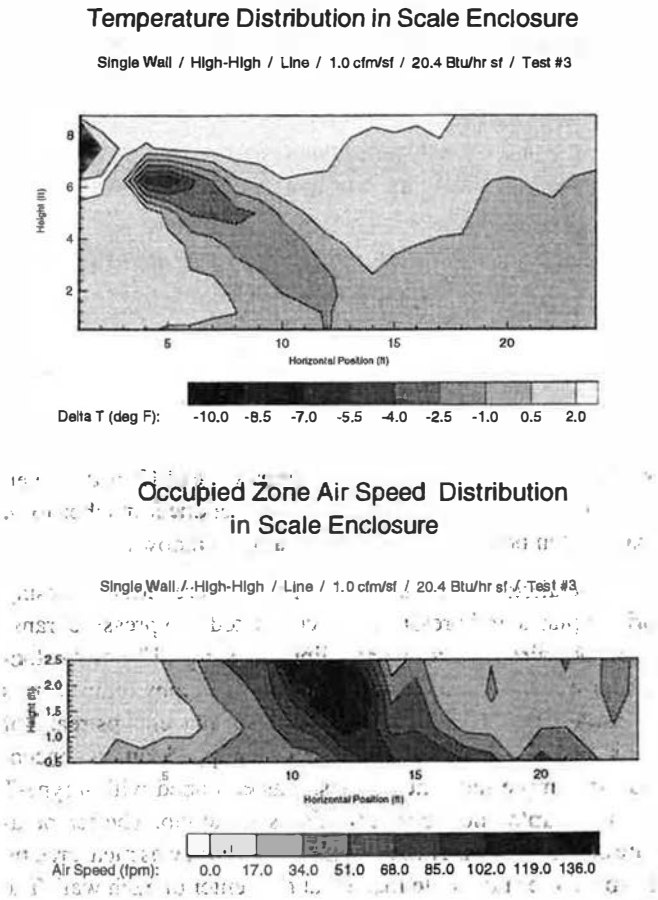

Figure 8 *Temperature and velocity for single wall high-high configuration.*

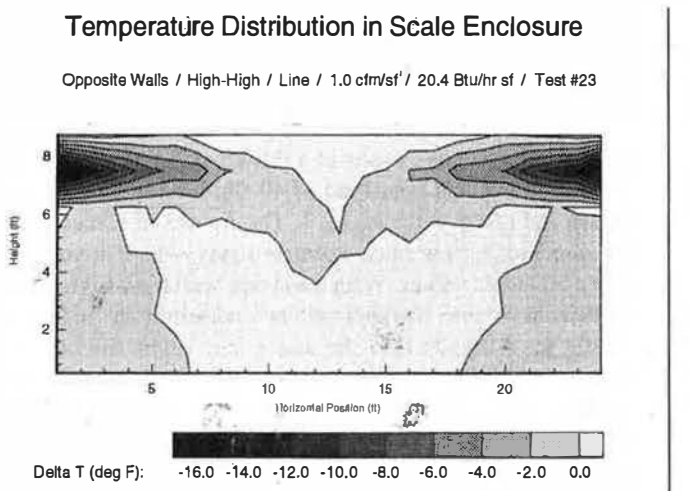

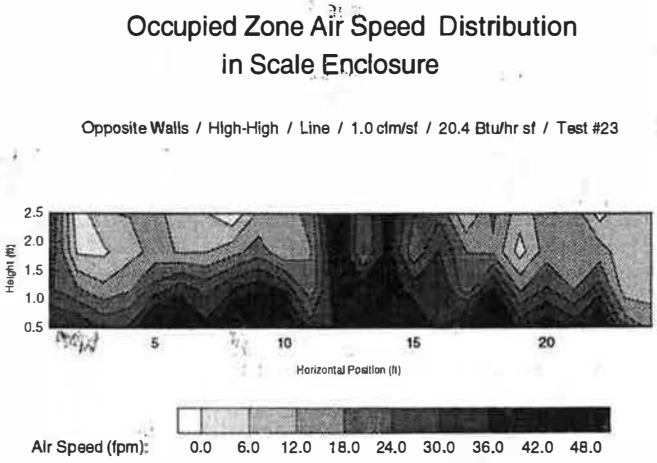

Figure 9 *Temperature and velocity for opposite wall high-high configuration.*

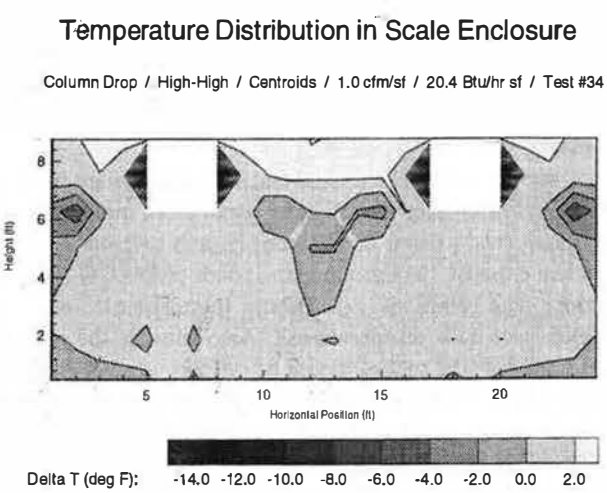

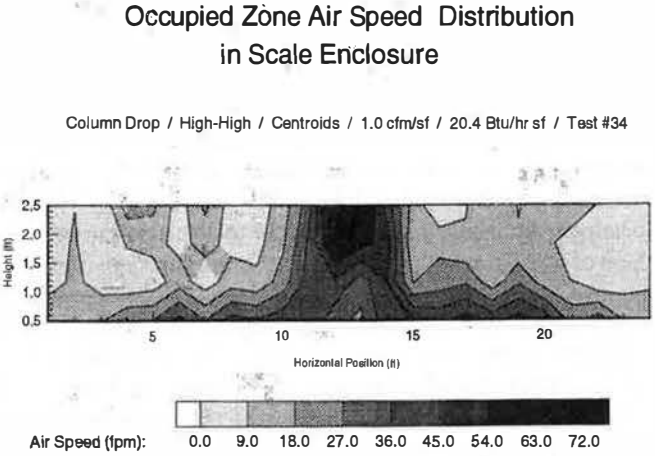

Figure 10 *Temperature and velocity for column drop high-high configuration.*

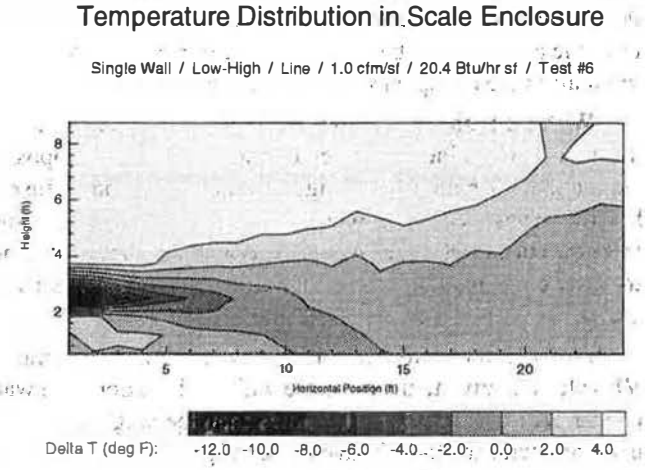

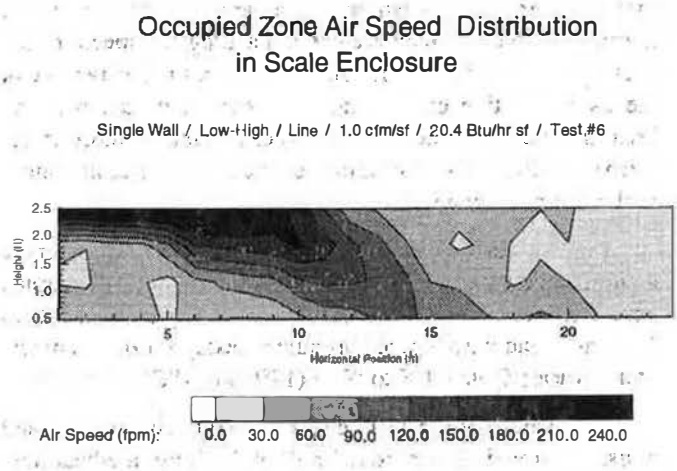

Figure 11 *Temperature and velocity for single wall low-high configuration.*

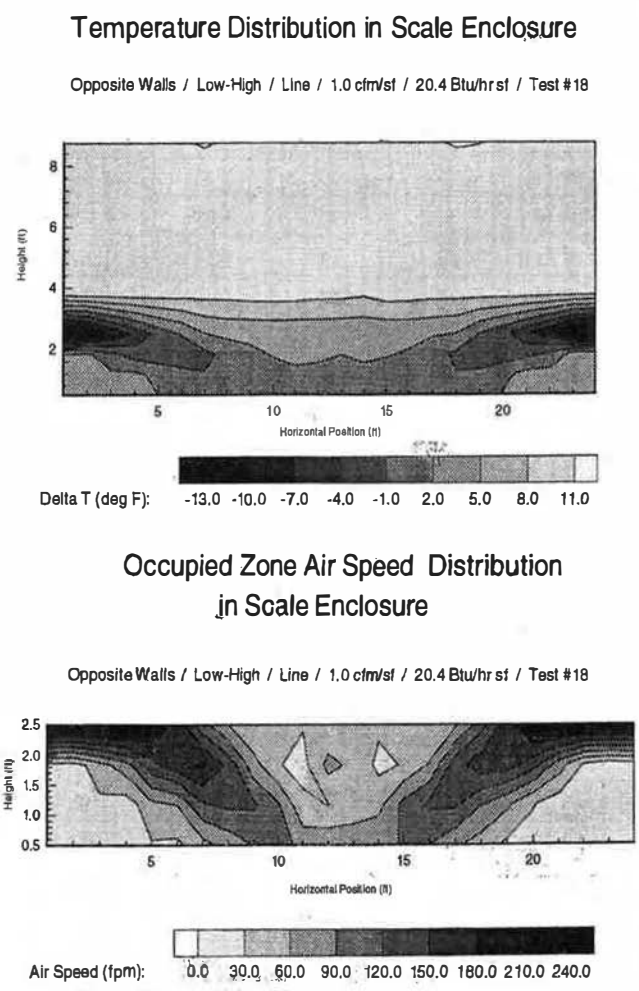

***Figure 12** Temperature and velocity for opposite wall low-high configuration.*

The ventilation and thermal comfort indices. ppd-1, ppd-2, TE, and VE, are tabulated in Tables 4 through 7 for the ten diffuser configurations for each of the four flow rate and heat load combinations. Also tabulated are the diffuser plane normalized average temperature and average airspeed for the occupied zone. The ventilation effectiveness is the average of the 24 ventilation effectiveness measurements taken at the breathing height in the diffuser plane. The temperature effectiveness is found from the area weighted average temperature in the occupied zone.

As the supply airflow rate is increased, the average airspeed increases correspondingly. The average occupied zone airspeeds varied from 25 fpm to 290 fpm (0.12 m/s to 1.47 m/s), and the average normalized occupied zone temperatures varied from 64°F to 80°F (18°C to 27°C).

The ventilation effectiveness has some interesting and consistent trends that persist for all of the flow rate/heat load combinations. The largest ventilation effectiveness occurred with the low-high configuration with values above 1.6, followed by the high-high configuration with values in the

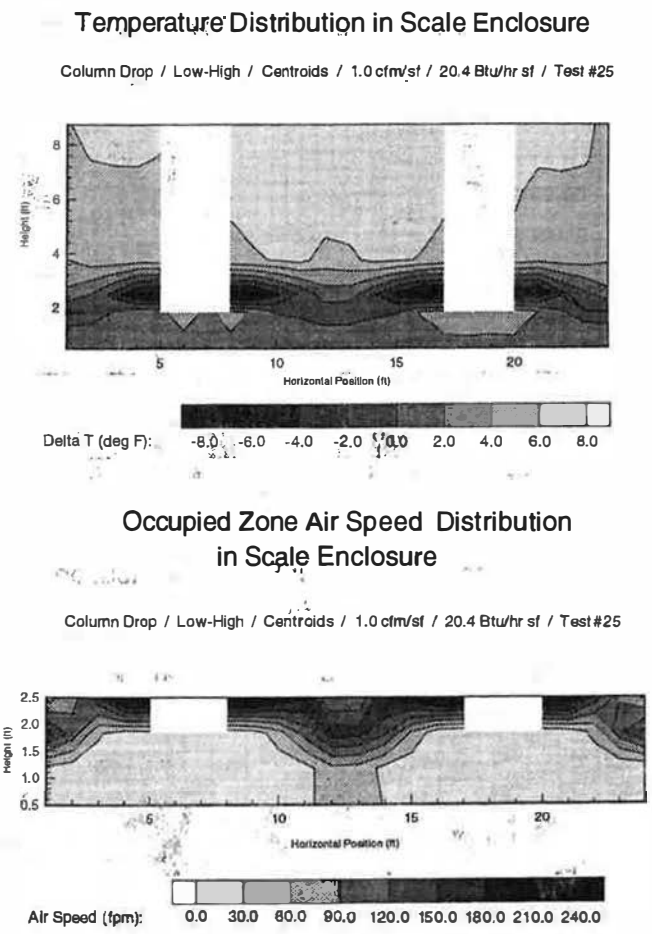

***Figure 13** Temperature and velocity for column drop low-high configuration.*

range from 1.0 to 1.2. The low-low configuration had values of about 1.0.

The higher VE values for the low-high configuration are due to two factors. The low supply delivers fresh air directly to the occupied zone. The high return causes the ventilation flow to be in the same direction as the natural convection flow from the cubes so that the mixing of the contaminant with the room air in the occupied zone is reduced.

With the high-high configuration, the round diffuser had the highest VE values, followed by the column drop, opposite wall, and the single wall configurations. The round diffusers had the lowest occupied zone velocities, so the process flow from the cubes was not as well mixed with the supply air, and thus, the contamination could migrate upward out of the occupied zone to the high return diffusers.

For all of the configurations, the column drop had higher VE values relative to the opposite wall, and the opposite wall configuration had higher VE values than the single wall. For example, with the 2-40 high-high configuration, the column drop VE was 1.15, the opposite wall was 1.10, and the single wall 1.00. This indicates that as the number of supply diffusers increases, the ventilation effectiveness increases. This result is

TABLE 4
Results for Test Configurations of 1.0 cfm/ft² and 20.4 Btu/h·ft²

Diffuser Type	Inlet	Exhaust	T_{oz} °F (°C)	V_{oz} fpm (m/s)	PPD-1	PPD-2	TE	VE
Round	High	High	67 (19)	25 (0.13)	13	26	1.14	1.20
Column Drop	High	High	72 (22)	35 (0.18)	5	39	1.09	1.06
Opposite Walls	High	High	77 (25)	42 (0.21)	13	58	1.11	1.14
Single Wall	High	High	78 (25)	30 (0.15)	18	63	1.12	1.09
Column Drop	Low	High	66 (19)	55 (0.28)	40	18	1.47	1.62
Opposite Walls	Low	High	74 (23)	64 (0.32)	5	44	1.43	2.18
Single Wall	Low	High	69 (20)	86 (0.44)	21	25	1.56	1.18
Column Drop	Low	Low	64 (18)	55 (0.28)	63	13	1.12	1.17
Opposite Walls	Low	Low	75 (24)	58 (0.29)	6	48	1.35	1.31
Single Wall	Low	Low	74 (23)	71 (0.36)	44	57	0.96	0.93

TABLE 5
Results for Test Configurations of 2.0 cfm/ft² and 20.4 Btu/h·ft²

Diffuser Type	Inlet	Exhaust	T_{oz} °F (°C)	V_{oz} fpm (m/s)	PPD-1	PPD-2	TE	VE
Round	High	High	65 (18)	38 (0.19)	32	17	1.28	1.19
Column Drop	High	High	71 (22)	43 (0.22)	7	35	1.09	1.18
Opposite Walls	High	High	76 (24)	46 (0.23)	9	54	0.99	1.02
Single Wall	High	High	73 (23)	78 (0.39)	6	38	0.95	0.96
Column Drop	Low	High	73 (23)	120 (0.61)	9	36	1.49	1.91
Opposite Walls	Low	High	72 (22)	140 (0.71)	11	34	1.64	1.65
Single Wall	Low	High	68 (20)	170 (0.86)	41	19	0.98	1.01
Column Drop	Low	Low	66 (19)	110 (0.56)	60	15	1.02	1.05
Opposite Walls	Low	Low	68 (20)	140 (0.71)	42	18	1.06	0.99
Single Wall	Low	Low	76 (24)	180 (0.91)	5	38	0.93	0.99

TABLE 6
Results for Test Configurations of 2.0 cfm/ft² and 40.8 Btu/h·ft²

Diffuser Type	Inlet	Exhaust	T_{oz} °F (°C)	V_{oz} fpm (m/s)	PPD-1	PPD-2	TE	VE
Round	High	High	76 (24)	50 (0.25)	8	53	0.84	1.20
Column Drop	High	High	76 (25)	50 (0.25)	7	52	1.15	1.15
Opposite Walls	High	High	78 (26)	56 (0.28)	16	63	1.09	1.10
Single Wall	High	High	82 (28)	96 (0.49)	35	76	1.00	1.00
Column Drop	Low	High	69 (21)	120 (0.36)	30	24	1.72	1.84
Opposite Walls	Low	High	73 (23)	150 (0.76)	9	37	1.69	1.84
Single Wall	Low	High	77 (25)	160 (0.81)	6	52	1.25	1.33
Column Drop	Low	Low	80 (27)	120 (0.61)	18	65	1.08	1.13
Opposite Walls	Low	Low	71 (22)	140 (0.71)	15	31	1.05	1.02
Single Wall	Low	Low	78 (26)	170 (0.86)	8	57	0.95	0.97

TABLE 7
Results for Test Configurations of 3.0 cfm/ft² and 40.8 Btu/h·ft²

Diffuser Type	Inlet	Exhaust	T_{oz} °F (°C)	V_{oz} fpm (m/s)	PPD-1	PPD-2	TE	VE
Round	High	High	72 (22)	65 (0.36)	7	36	0.82	1.21
Column Drop	High	High	77 (25)	67 (0.34)	9	55	1.14	1.17
Opposite Walls	High	High	—	—	—	—	0.98	1.04
Column Drop	Low	High	72 (22)	175 (0.89)	13	33	1.61	1.83
Opposite Walls	Low	High	72 (22)	220 (1.11)	15	32	1.54	1.68
Single Wall	Low	High	77 (25)	290 (1.47)	5	50	1.01	1.00
Column Drop	Low	Low	71 (22)	170 (0.86)	24	27	1.14	1.04
Opposite Walls	Low	Low	71 (22)	200 (1.02)	19	30	1.14	1.02
Single Wall	Low	Low	78 (26)	250 (1.27)	7	56	1.00	0.97

reasonable, since with an increased number of diffusers, fresh air is delivered to more locations in the occupied zone.

In general, for a given configuration, the ventilation efficiency increased when the heat load was increased and/or the flow rate decreased. This occurred because the increased heat load created a more intense convection plume above each industrial process. These intensified plumes were able to transport contaminant upward and to the exhaust with less mixing. With increased supply flow rate, there was increased mixing of the supply flow with the process flow, resulting in higher contaminant concentrations in the occupied zone.

The temperature effectiveness varies from 1.72 for the low-high configurations to 0.93 for the low-low configurations, with most values around 1.05. Even though they indicate the performance of different aspects of the convective processes in the test room, the temperature effectiveness values track very closely to the ventilation effectiveness values.

The thermal comfort results are dependent on the flow rate/load combination. The results are complementary in the sense that a configuration acceptable for a ppd-1 condition is not acceptable for a ppd-2 condition and vice versa. Most of the configurations produced acceptable results for the ppd-1 condition and unacceptable conditions for the ppd-2 condition. For example, in the 1-20 tests, all of the diffuser configurations are acceptable for a ppd-1 condition with the exception of the column drop low-low, column drop low-high, and the single wall low-low. However, at the ppd-2 condition, only the column drop low-low and column drop low-high configurations are acceptable. With increased activity and clothing levels, the only diffuser configurations that performed acceptably were those that delivered supply air directly to the occupied zone.

These results are reasonable since the ISO thermal comfort model predicts that to maintain thermal comfort as the clothing and activity level is increased, an increase in the airspeed and/or a decrease in the occupied zone temperature is required. If the occupied zone temperature is too low and/or the airspeed too high, the ppd-1 conditions are not acceptable. Likewise, if the occupied zone temperature is too high and/or the airspeed too low, the ppd-1 conditions are not acceptable.

SUMMARY AND CONCLUSIONS

The evaluation of the ventilation effectiveness and thermal comfort for various industrial ventilation schemes has been carried out by scale model experimentation. Forty experiments involving ten ventilation arrangements, each with three supply airflow rates and two possible industrial process heat loads, were performed. Measurements of airspeed, temperature, and contaminant concentration allowed the thermal comfort and contaminant removal to be quantified using the ISO comfort standard 7730 and the ventilation effectiveness indices, respectively. Archimedes number scaling was used to convert the small-scale measurements to full-scale conditions.

The largest ventilation effectiveness occurred with the low-high configuration, with values above 1.6, followed by the high-high configuration with values in the range from 1.0 to 1.2. The low-low configuration had values of about 1.0. Increasing the number of diffusers in the occupied zone increased the ventilation effectiveness. For a given configuration, the ventilation efficiency generally increased when the heat load was increased and/or the flow rate decreased. With increased activity and clothing levels, the only diffuser configurations that performed acceptably were those that delivered supply air directly to the occupied zone. Most of the diffuser configurations produced acceptable results for the ppd-1 condition and unacceptable conditions for the ppd-2 condition.

ACKNOWLEDGMENTS

This work was produced under ASHRAE Research Project 811, under the direction of TC 5.8. The project monitoring subcommittee, chaired by Gerhard Knutson, provided valuable guidance.

REFERENCES

Chan, W., Y. Wong, and G. Fong. 1993. Experimental studies of air distribution in a high-ceilinged space. ASHRAE Transactions 99 (2): 158-162.

Chen, Q., A. Moser, and P. Suter. 1992. A numerical study of indoor air quality and thermal comfort under six kinds of air diffusion. *ASHRAE Transactions* 98 (1): 203-217.

Fissore, A., and G. Liebecq. 1991. A simple empirical model for predicting velocity distributions and comfort in a large slot-ventilated space. *ASHRAE Transactions* 97 (2): 1087-1095.

Heiselberg, P. 1996. Room air and contaminant distribution in mixing ventilation. *ASHRAE Transactions* 102 (2): 332-339.

Int-Hout, D., 1990. Thermal comfort calculations—A computer model. *ASHRAE Transactions* 96(1): 840-844.

Irwin, D.R., and R.W. Besant. 1994. Contaminant removal efficiencies in a model barn using a displacement ventilation system and a conventional supply slot system. *ASHRAE Transactions* 100(2): 1021-1033.

ISO. 1984. *ISO Standard 7730-84, Moderate thermal environments—Determination of PMV and PPD indices and specification of the conditions for thermal comfort.* Geneva: International Standards Organization.

Schlicting, H. 1979. *Boundary layer theory*, 7th ed. New York: McGraw-Hill.

Skaret, E., and H. Mathisen. 1983. Ventilation efficiency—A guide to efficient ventilation. *ASHRAE Transactions* 89(2B): 480-495.

Timmons, M.B. 1984. Use of physical models to predict the fluid motion in slot ventilated livestock structures. *Transactions of the ASAE* 27(2): 502-507.

Yaghoubi, M., K. Knappmiller, and A. Kirkpatrick. 1995. Three-dimensional numerical simulation of air contamination dispersal in a room. *ASHRAE Transactions* 101(1): 1031-1040.

Zhang, J.S., G.J. Wu, L.L. Christianson. 1993. A new similitude modeling technique for studies of nonisothermal room ventilation flows. *ASHRAE Transactions* 99(1): 129-138.